Fullwave Analysis of Transverse and Longitudinal Couplings in Silicon RFIC. Effect of Buried Diffusions.

S. Wane*, D. Bajon**, H. Baudrand* and P. Gamand***

*ENSEEIHT 2 rue Camichel 31071 Toulouse-France wane@len7.enseeiht.fr , **SUPAERO 10 av. Ed. Belin, 31055 Toulouse-France ***Philips Semiconductors 2 rue de la girafe - 14079 Caen -France

***Abstract* — Couplings in Silicon based RFIC result from the combination of the effects of the substrate resistivity, homogenous and localized buried diffusions as well as metallic losses. A fullwave analysis is performed and longitudinal and transverse coupling coefficients are defined from a generalized equivalent circuit. Concurrently, considerable improvement of isolation performances are demonstrated by inserting localized buried diffusions.**

I. Introduction

RFIC on silicon present thin layers stacks including, in addition to the substrate, diffusion and epitaxial layers with different doping levels, as well as induced space charge [1] and oxide layers, all of them contributing to the coupling between signal coplanar strip lines. Schematic of this situation is given in Fig.1 with the typical parameters values considered herein.

Thin layers stacks require, to fullwave analysis in the spatial domain, refined discretizations while in spectral domain, they are directly involved in the building of the integral operators since they are homogeneous. To account for non homogeneous layers resulting from localized diffusions, in the following , a specific extension of the transverse resonance technique is performed.

The usually penalising time searching in the complex domain of propagation constants, thought to be the most significant central processing delay, is avoided owing to an optimised home-made complex roots searching algorithm. From this fullwave analysis, a general equivalent circuit in which two two-ports distinguish longitudinal and transversal couplings is introduced to traduce competitive effects between metallic losses, buried diffusions and substrate doping levels. Intrinsic coupling coefficients D_L and D_T, associated respectively to the longitudinal and transversal couplings, are defined from the directivities of the two two-ports, independently of the loading conditions.

II. Fullwave Analysis and Discussion

Since spectral domain analysis handles spectral expansion of the integral operators [2], a key point of the analysis is the building of a bi-othogonal basis functions since the usual transverse TE and TM expansion functions do not fulfill orthogonality conditions in the complex case. Account for inhomogeneous stack is made possible by introducing in the integral formulation spatially varying surface impedance boundary conditions describing the doping level profile.

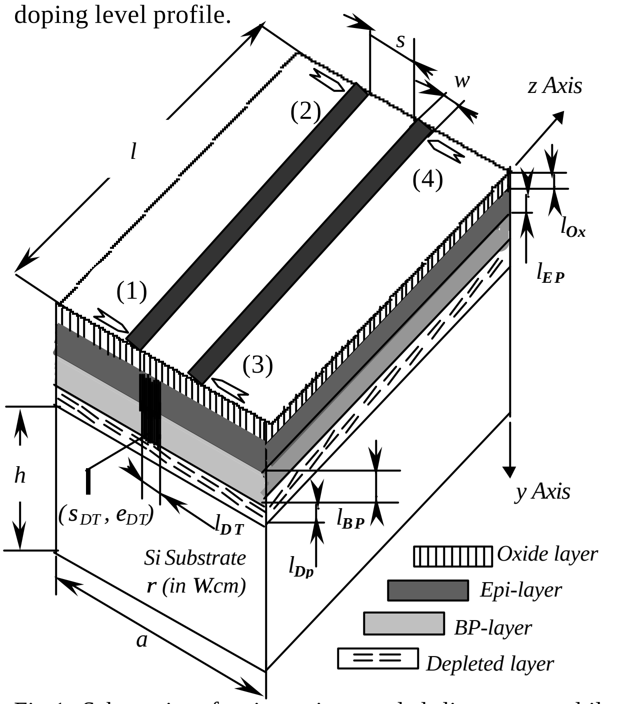

Fig.1 Schematic of microstrip coupled lines on multilayer structure on silicon substrate with buried diffusion – h=400 µm, l_{Dp} = 1 µm, s = 20 µm, w = 10 µm, l_{BP} = 1.5 µm, l_{EP} = 0.8 µm, l_{Ox} = 1.8 µm , σ_{DT} = 320 S/m, σ_{EP} = 200 S/m.

A. *Effects of the buried diffusion.*

Although their influence on the attenuation is more considerable for the odd mode, all over the substrate resistivity range, the metallic losses are seen responsible, for the even mode, in Fig.2-a, of an offset of the attenuation of around 3 10^{-2} Np/mm in region I, 10^{-2} Np/mm in region II and 2 10^{-2} Np/mm in the slow wave region.

0-7803-6540-2/01/$10.00 (C) 2001 IEEE

In fact, as early reported in the case of microstrip [3-4], there are, in regard to the substrate resistivity, basically, three operating regions : the slow-wave region, in the range of 10^{-2} to 5 Ω.cm at 2 GHz as attested by the slowing factor Fig. 2-b, between the metallic region (region I) and the lossy dielectric region (region II). Conversely to the attenuation, in each region, the slowing factor is monotonous.

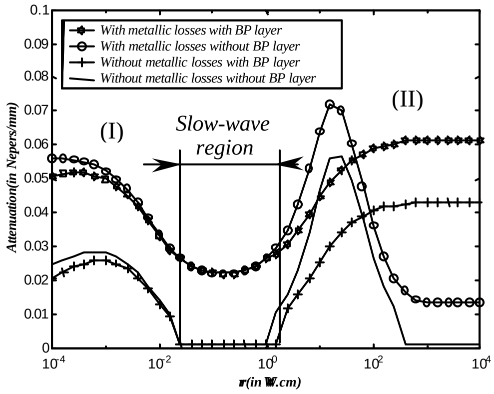

(a)

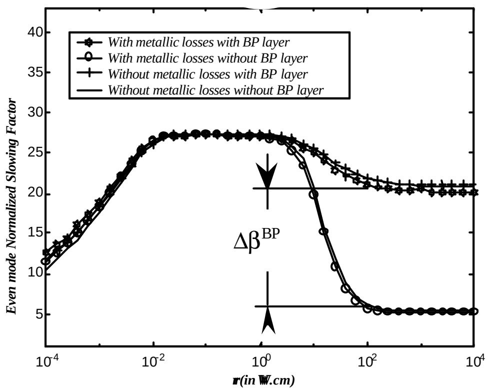

(b)

Fig.2 Effects of the metallic losses and of the BP layer on even mode attenuation constant (in Np/mm) (a) and normalised slowing factor (b) against the substrate resistivity at 2 GHz.

- In the slow-wave region, the BP layer, whose resistivity is in the substrate resistivity range (Fig.1), has no effect on the slowing factor and the attenuation which reach respectively their maximum and minimum values. In this region weak isolation performances have to be expected because of the disparity between the even and odd mode slowing factors (Fig.2-b). The analysis of the Poynting vector distribution, both in the slow-wave region and in the lossy dielectric domain, exhibits lower energy concentration between the lines in the slow-wave region (Fig.5-a). Thus, in the slow-wave region where the electric field is more attenuated than the magnetic field, the lines are more coupled than in the dielectric domain.

- In the region I, the BP-layer, which acts as a resistive layer in parallel with the substrate and the metallic losses, reduces the attenuation constant while, an increase of the normalized slowing factor is noticed as the substrate resistivity increases (Fig.2-a).

- In the region II, the BP-layer, screening the effects of the substrate resistivity, considerably increases the even mode normalized slowing factor and attenuation constant. Without BP-layer, significative decrease of the normalized slowing factor is obtained as the substrate resistivity becomes greater. For a 10^4Ω.cm substrate resistivity, the slowing factor and the attenuation of the even mode are four times less than with the BP-layer. Buried diffusions in Fig. 3, are seen deeply disturbing the proximity effect and finally, introducing a transverse coupling : the S_{13} parameter with BP layer requires a five time wider lines spacing to attain the same isolation level as without BP layer.

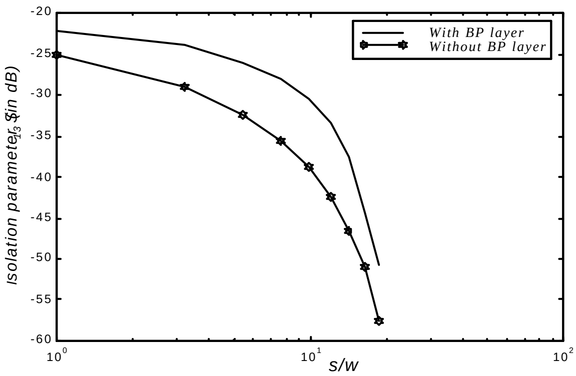

Fig.3 Effects of the lines spacing at 2 GHz, on the isolation parameter S_{13} with and without BP layer for $\rho = 10^4$ Ω.cm..

B. Effects of localised buried diffusion.

The BP-layer decreasing the isolation performances (with important gap $\Delta\beta^{BP}$), it would be interesting to interrupt it with a localized buried diffusion to improve the structure isolation performances.

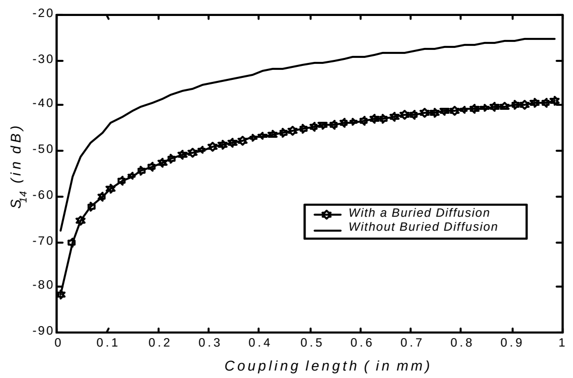

Fig.4 Effect of a buried diffusion of width $l_{DT} = 10$µm ($\varepsilon_{DT}= 4.5$ and $\sigma_{DT} = \infty$) on the coupling S_{14} at 2 GHz for $\rho = 20$ Ω.cm.

The coupling parameter S_{14} using a 50 Ω normalizing impedance for a coupling length up to *1*mm is shown in Fig.4, demonstrating an improvement of 15 dB of the isolation performances at 2 GHz.

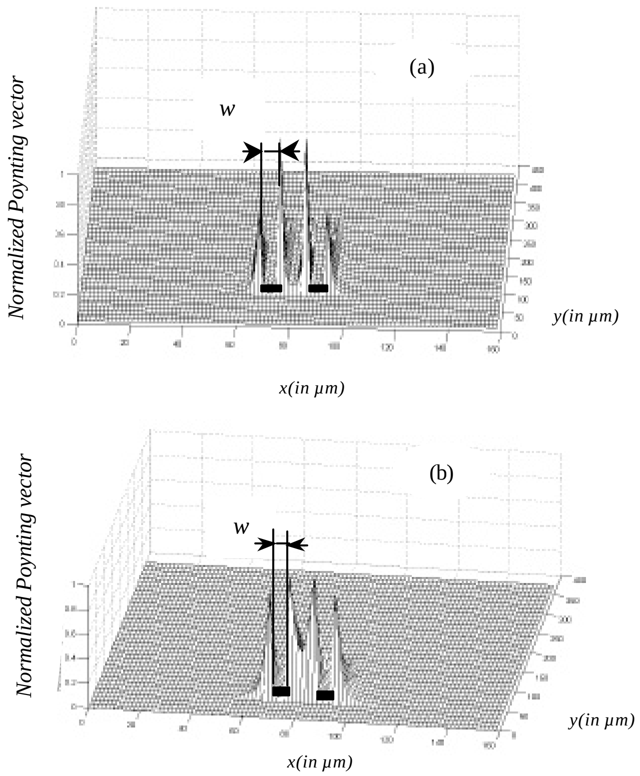

Fig.5 Even mode Normalized Poynting vector distribution in the overall structure in the slow-wave region (ρ = 0.1 Ω.cm) (a) and in the lossy dielectric region (b) at the frequency 2 GHz ($\rho = 10^4$ Ω.cm).

III. Extraction Of Quasi-TEM Representations

For CAD purpose it is convenient to give the quasi-TEM ladder circuit representation of an infinitesimal line length with serial impedance $Zs = Z_c\,\gamma$ and parallel admittance $Yp = \gamma / Z_c$ which real and imaginary parts are respectively *R*, *G* and *L*, *C*, $\gamma = \alpha + j\beta$ being the propagation constant and Z_c the characteristic impedance, both issued from the fullwave analysis. This extraction procedure circumvents the main question for a quasi-TEM approach which would be to decide how the losses due to the substrate and the buried diffusion have to be distributed between the serial parameter R and the parallel one G. However, this extraction is tributary to the chosen definition of the characteristic impedance which will drive the condition for the real parts of Z and Y to be positive. This condition is readily derived as :

$$t_g \ge t_{Z_c} \text{ with } t_g = \left|\frac{a}{b}\right| \quad \text{and} \quad t_{Zc} = \left|\frac{\Im m(Z_c)}{\Re e(Z_c)}\right| \qquad (1)$$

From the above analysis, the ratio τ_γ takes its minimum value in the slow-wave region, in which, accordingly to the adopted definition of the characteristic impedance, negative real part for Zs or Yp can be encountered.

General equivalent circuit of coupled lines

Performing this extraction for both the even and the odd modes, the eight parameters related to the real and imaginary parts of $\gamma_{even,odd}$ and $Z_{Ceven,odd}$ completely characterizing the coupled lines, the resulting electrical representation should also involve eight elements. Usually, on free loss substrates, coupling is electrically represented by only the mutual inductance *M* and the inter-metal capacitance C_c in Fig. 6-a given by :

$$M = \frac{1}{2}\Im m(Z_{even} + Z_{odd}) \quad \text{and} \quad C_c = \frac{1}{2}\Im m(Y_{even} + Y_{odd}) \qquad (2)$$

while metallic losses are accounted in a serial resistance indifferently determined from the odd or the even mode configuration. In the present case, the situation is quite different since the real parts of Z_{even} and Z_{odd} are notably different due to the competition between substrate resistivity, buried diffusion and metallic losses. Accordingly, we present an eight parameters electrical representation of coupled lines involving, no four impedances, but two symmetrical two-ports as shown in Fig. 6-b, one relative to the longitudinal coupling (Z_L, Z_L’) and the other one relative to the transverse coupling (Y_T, Y_T’). This electrical representation is moreover suitable for the case of structures without back metallization as shown in Fig. 6-b.

The elements Z_L, Z_L’, Y_T and Y_T’ are obtained by identification with the even and odd modes parameters :

$$Z_L = Z_{even}, \quad Y_T = Y_{even}, \quad Z_L' = 2\frac{Z_{even}Z_{odd}}{Z_{even} - Z_{odd}} = 2z'$$

$$\text{and} \quad 1/Y_T' = \frac{(c - Z_{even})k}{k - (c - Z_{even})} \qquad (3)$$

$$\text{with} \quad c = \frac{z'(Z_{even} - Z_{odd})}{z' - Z_{even} + Z_{odd}} \quad \text{and} \quad k = z' // (1/Y_T)$$

From the directivities of these two-ports, the two intrinsic coupling coefficients $D_L = Z_{12} / Z_{11}$ and $D_T = Y_{12} / Y_{11}$ defined from the elements Z_{ij} and Y_{ij} of the impedance and admittance matrix of respectively Q_L and Q_T in Fig. 6-b are given, in terms of Z_L, Z_L’, Y_T and Y_T’ by :

$$D_L = \frac{1}{1 + 2Z_L'/Z_L} \quad \text{and} \quad D_T = \frac{1}{1 + Y_T/Y_T'} \qquad (4)$$

such that their magnitude tends towards zero as respectively $|Y_T'|$ tends to zero and $|Z_L'|$ to infinity.

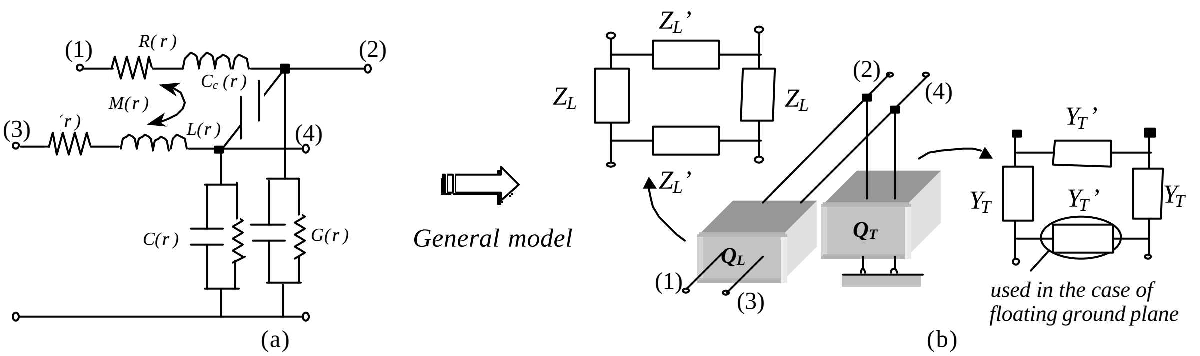

Fig.6 Quasi-TEM model of symmetrical microstrip coupled lines (a) and general electromagnetic equivalent scheme of interconnects in the symmetrical case (b)

These intrinsic coupling coefficients characterize the coupling independently of the loading charges of the lines as well as the mismatch towards the reference impedance used in the definition of the scattering parameters. D_L and D_T coefficients are expected to be less dependent to the definition of the characteristic impedance unlike the usual quasi-TEM parameters M and C_c usually introduced.

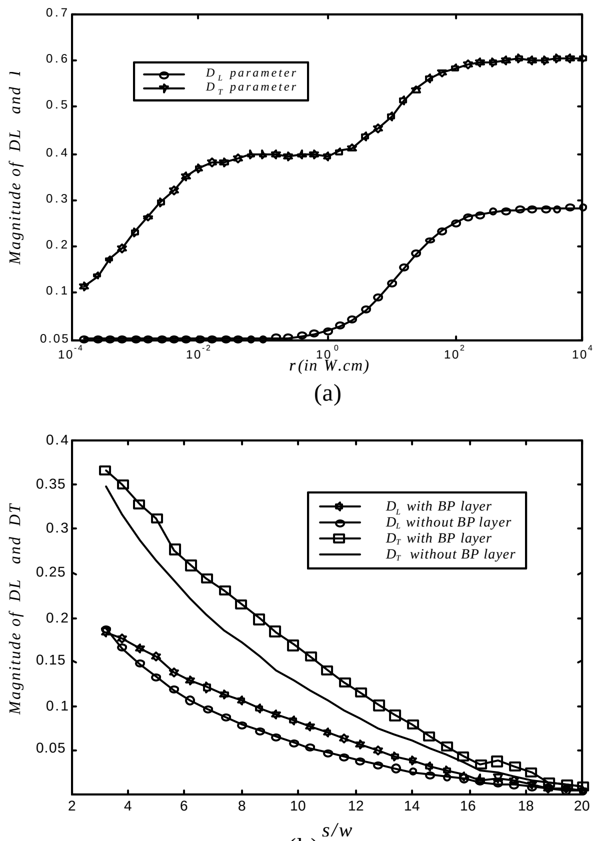

Fig.7 Magnitude of the Coupling Intrinsic Coefficients D_L and D_T against the substrate resistivity (a) and against the lines spacing (b) at 2 GHz from the general equivalent circuit in Fig.6-b.

Relatively to the considered structures, in Fig.7, the longitudinal coupling is notably less than the transverse one, both of them increasing for substrate resistivities up to 10^2 Ω.cm and in presence of buried diffusions.

IV. CONCLUSION

From fullwave analysis, buried diffusions have been seen responsible for a weakening of isolation performances. A complete equivalent network for coupled lines has been introduced which allows the definition of longitudinal and transverse intrinsic coupling coefficients and applies also to no ground backed structures. A spatially varying doping level profile included in an integral formulation in the spectral domain describes localized buried diffusions. The introduction of a localized buried diffusion has demonstrated significant isolation improvement.

REFERENCES

[1] A.C. Reyes, S. M. EL-Ghazaly, S. Dorn, M. Dydyk, D. Schroder, " High-resistivity Si as a Microwave Substrate" *Electronic Components and Techn. Conf.* 1996 pp 382-391

[2] F.Bouzidi, H.Aubert, D.Bajon and H.Baudrand, "Equivalent network representation of boundary conditions involving generalised trial quantities - Application to lossy transmission lines with finite metallisation thickness", *IEEE Trans. on Microwave Theory and Techniques,* volume 45, n° 6, p 869-876, June 1997

[3] Y. Fukuoka Y. Shih and T. Itoh, "Analysis of slow-wave coplanar waveguide for monolitic integrated circuits," *IEEE Trans. on Microwave Theory and Techniques,* vol. MTT-31 pp. 567-573, July 1983.

[4] Young Rack Kwon , Vincent M. Hietala and Keith S. Champlin, "Quasi-TEM Analysis of "Slow-Wave" Mode Propagation on Coplanar Microstructure MIS Transmission Lines", *IEEE Trans. on Microwave Theory and Techniques,* vol. MTT- 35, n° 6, p 545-551, June 1987.